RSC Advances

PAPER

View Article Online
View Journal | View Issue

Cite this: *RSC Adv.*, 2021, **11**, 18084

Synthesis and biological evaluation of biotin-conjugated *Portulaca oleracea* polysaccharides

Qianqian Han,[ab] Lirong Huang,*[c] Qiang Luo,[ab] Ying Wang,[ab] Mingliang Wu,[a] Shixin Sun,*[a] Hongmei Zhang[a] and Yanqing Wang *[a]

Received 20th March 2021
Accepted 11th May 2021

DOI: 10.1039/d1ra02226a

rsc.li/rsc-advances

Biotinylated *Portulaca oleracea* polysaccharide (Bio-POP) conjugates were successfully prepared by the esterification reaction. The biotinylated polysaccharide products were an off-white powder with an average degree of substitution of 42.5%. After grafting biotin onto POP, the thermal stability of Bio-POP conjugates was much higher than that of POP and the surface topography of Bio-POP was a loose and porous cross-linked structure. The cytotoxicity assay *in vitro* demonstrated that POP, biotin, and Bio-POP conjugates exhibited different cytotoxicity to HeLa, MCF-7, LO-2, and A549, in particular POP inhibited the growth of the A549 cell line more than other cell lines. The nuclear staining method demonstrated that Bio-POP conjugates can interfere with the apoptosis of A549 cells to some extent and the immunofluorescence staining photograph illustrated that Bio-POP conjugates induced A549 cells to exhibit immune activity. Therefore, the combination of biotin and *Portulaca oleracea* polysaccharides had immune synergistic therapeutic effects on A549 cells and can be applied in the field of anti-tumor conjugate drugs.

1. Introduction

Cancer has the highest morbidity and mortality among several human diseases worldwide.[1] At present, surgery, radiotherapy, and chemotherapy are the three most commonly used methods to treat cancer. Chemotherapy is a type of clinical treatment method that uses chemical or biological agents to prevent tumour cell proliferation and metastasis, and even kill the tumour cells.[2,3] Drugs based on polysaccharide complexes have emerged, which are widely used by human beings due to their special applications in the biomedical field.[4] Owing to the potential biological activities of plant polysaccharides, such as immune regulation, anti-tumour activity, antiviral activity, hypoglycemic activity, antioxidant activity, and so on,[5] the activity of plant polysaccharides and their complexes are the current research hotspot.[6] Recently, increasing amounts of literature have testified that polysaccharides separated from botanical sources have not only anti-cancer activities but also biological compatibility and biological degradation, which has attracted considerable attention.[7]

In recent decades, the research progress of polysaccharides-based drugs had been rapid, which promoted the discovery of a variety of chemotherapy drugs.[8] Numerous potent drugs with sparingly low water-solubility were difficult to be administrated by intravenous injection, which limited their clinical application. However, polymer delivery systems had been used successfully for hydrophobic drug delivery.[9,10] Chemotherapy drugs were usually lack of targeting and selectivity, which made them not only kill cancer cells but also normal cells.[11] The drug delivery system was used to improve the drug transmission efficiency and concentration to reach and act on the tumour site and reduce the toxic and side effects on the human body during the chemotherapy process.[12,13]

Moreover, polymerics can also circulate for a long time and preferentially accumulate in tumour sites *via* the enhanced permeability and retention (EPR) effect.[14,15] Active targeting technology has taken advantage of ligand-receptor, antigen–antibody, and other forms of molecular recognition to deliver particles or drugs to a specific location.[16] For instance, a variety of macromolecules and small organic molecules with special functions were composed of molecule tumour-targeting receptors (*e.g.*, biotin or folic acid).[17] For cancer therapy, active targeting components were particularly beneficial because they reduced or eliminated the possibility of delivering of potentially toxic drugs to healthy tissue.[18] The prodrug was connected by a linker to form a stable prescription. When it reached the cell, it could be affected by intracellular glutathione, enzymes or changed in pH value to release the prodrug, which acted on and inhibited the growth of cancer cells.[19]

Portulaca oleracea polysaccharides (POP) was a type of Chinese herbal medicine polysaccharides with biological

[a]*Institute of Environmental Toxicology and Environmental Ecology, Yancheng Teachers University, Yancheng City, Jiangsu Province, 224051, People's Republic of China. E-mail: asunshixin@163.com; wyqing76@126.com*

[b]*Chemistry and Chemical Engineering, Nanjing University of Technology, Nanjing City, Jiangsu Province, 210009, People's Republic of China*

[c]*Cardio-Thoracic Surgery, Yancheng First People's Hospital, Yancheng 224006, China. E-mail: ychlr009@163.com*

activity, which was isolated from purslane.[20] In addition, POP also had varieties of biological functions, such as the antioxidant activities,[21,22] the antiviral effect,[23] the hypoglycemic effect,[24] the immunomodulatory effect,[25,26] the antifungal activity,[27] and the anti-tumour activities.[28] On the other hand, *Portulaca oleracea* polysaccharides had the advantages of good stability, modifiable groups, good biocompatibility, and biodegradability. There were few reports on the synthesis of new chemotherapeutic drugs with *Portulaca oleracea* polysaccharides as the carbon skeleton. Plant polysaccharides also had medicinal functions. Therefore, *Portulaca oleracea* polysaccharides were selected as the carrier for functional modification. Many researchers had learned from the research reports that the biotin receptors were overexpressed on the surface of most cancer cells, so synthetic biotin can be preferentially recognized as terminal conjugates.[29,30] The chemical structure of biotin has a carboxyl group at the end, which can react with a variety of chemical groups after activation and has high chemical activity.

In this study, *N*,*N*′-carbonyl diimidazole was utilized as a coupling agent to modify *Portulaca oleracea* polysaccharides by biotin, and a new anticancer coupling agent was synthesized. The product of Bio-POP conjugates was characterized by varieties of physicochemical techniques, for example, determination of crystallinity, thermal stability, morphology, *etc.* In order to explore the inhibitory effects of POP, biotin, and Bio-POP conjugates on the growth of four cells, the MTT reduction assay was used to determine the IC_{50} for 48 h. A549 cells were cultured with samples of different concentrations and observed under an inverted fluorescence microscope. Besides, the release of calreticulin in A549 cells was observed by immunoassay and confocal fluorescence microscope.

2. Materials and methods

Materials

N,*N*′-Carbonyl diimidazole (CDI), biotin, trimethylamine (TEA) and 3-(4,5-dimethyl-thiazol-2-yl)-2,5-diphenyl-tetrazolium bromide (MTT) were procured by Aladdin. *Portulaca oleracea* polysaccharides (POP) was purchased from Ciyuan Biotechnology, Shanxi. RPMI-1640 medium (RPMI), DMEM medium, trypsin–EDTA (0.5% trypsin, 5.3 mM EDTA tetrasodium) were procured from Biyuntian Biotechnology Co., Ltd. Fetal bovine serum (FBS) was obtained from Shanghai ExCell Biology Inc. Anti-Calreticulin antibody and Alexa Fluor® 488 were purchased from Abcam (Shanghai) Trading Co., Ltd. Other analytical grade chemicals were used reasonably in accordance with regulations.

Synthesis of biotinylated *Portulaca oleracea* polysaccharides

The *Portulaca oleracea* polysaccharides was accurately weighed, dissolved in 100 mL distilled water, centrifuged at 8000 rpm for 0.5 h, filtered under reduced pressure, and dialyzed (MWCO: 3500 Da) by distilled water for three days. The soluble small molecules and insoluble substances were removed. Then the dialysate was put into a freeze-drying bottle, stored in a −20 °C refrigerator for at least 4 h, and then freeze-dried in a freeze-drying machine to obtain pretreated *Portulaca oleracea* polysaccharides.

Biotinylated *Portulaca oleracea* polysaccharides was synthesized and modified by similar reported methods.[31,32] The synthetic route of the final product was displayed in Fig. 1. Biotin (586 mg, 2.40 mmol) and CDI (324 mg, 2.00 mmol) were dissolved in 5.0 mL DMSO, which was activated at 50 °C for 12 h and nitrogen protection, was carried out at room temperature. The polysaccharides of *Portulaca oleracea* (480 mg) was completely dissolved in 15.0 mL dimethyl sulfoxide and then activated biotin solution added into the solution. Moreover, 200 μL TEA was added to regulate alkalinity, and then the reaction was conducted at 75 °C for 24 h. 180.0 mL of anhydrous ethanol was added to 20.0 mL of DMSO reacted solution. The centrifuge separation was then rinsed with 30.0 mL anhydrous ethanol, and the process was repeated twice. The gray-white solid particles were obtained after spinning and drying.

FT-IR spectroscopy analysis

The structure of the substance was identified by FT-IR spectroscopy, reflecting the type of functional group contained in the substance. Therefore, FT-IR spectroscopy (Bruker Vertex 80,

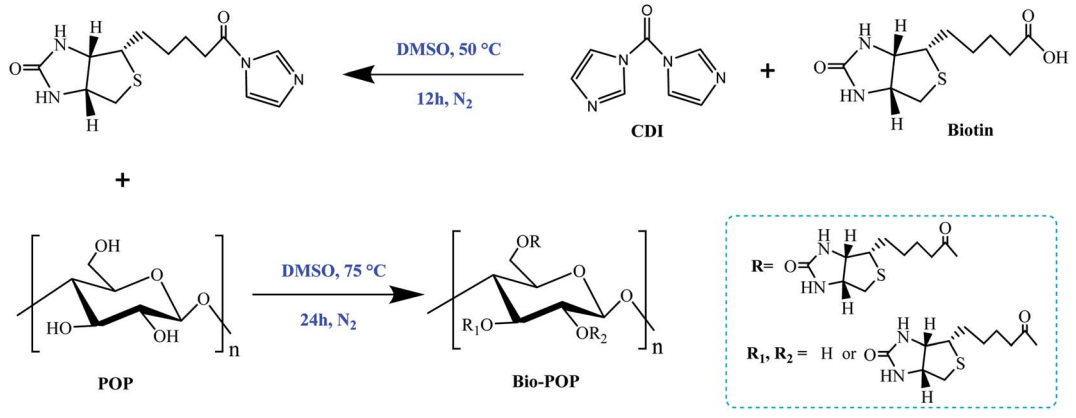

Fig. 1 The synthesis route of Bio-POP conjugates.

Switzerland) was used to detect the absorption of infrared rays by various functional groups and obtain FT-IR spectra. The FT-IR spectroscopy of raw materials and products were measured by the potassium bromide tablet method. Measurement requirement, which was taken solid material after freeze-drying, and the sample should not contain free water. The samples after completely freeze-dried were mixed with dry pure KBr to form a uniform powder suitable for measuring the frequency. The measurement results were taken in the range of 4000–500 cm^{-1} wavenumber.[33]

^{1}H NMR spectroscopy

^{1}H NMR spectra were collected using an AVANCE III HD 400 MHz (Bruker, Germany). A certain mass of biotin, POP and Bio-POP conjugates were respectively dissolved in 99.9% deuterium dimethyl sulfoxide (600 μL, DMSO-d_6) for ^{1}H NMR experiment which was performed with 16 MHz and 25 °C by nuclear magnetic resonance spectrometer. The MestReNova 12 software was used to analyze the data.[34]

Determination of degree of substitution (DS)

The degree of substitution (DS) of biotin in Bio-POP conjugates was defined as the coupling number was biotin on 100 anhydrous glucose residues. The DS used an inductively coupled plasma spectrometer (ICP-OES, PerkinElmer, Optima 4300 DV, USA) to determine the sulfur element (S) content in the Bio-POP conjugates, and then converts it to the degree of substitution of biotin by the following formula eqn (1). Specific methods: we accurately weigh 10 mg of Bio-POP conjugates, put it into a 10 mL volumetric flask, dissolved it with concentrated hydrochloric acid, and fixed the volume. The prepared solution was tested, and 100 mg L^{-1} standard sulfur solution was used as the standard sample. It was calculated specifically according to the formula eqn (1):

$$\mathrm{DS} = M_S/M_A \times 100 \quad (1)$$

where $M_S = (C_S \times V)/32$, $M_A = (W_{total} \times W_{biotin})/162$, $W_{biotin} = M_S \times 227.31$. M_S is the number of moles of sulfur element which is equal to the number of moles of biotin. M_A is the number of moles of anhydrous glucose residue. C_S is sulfur concentration determined by ICP (mg L^{-1}) and V is volumetric flask volume (mL). W_{total} and W_{biotin} are the total mass of the product to be tested and the total biotin residue mass of the product to be tested (mg).

X-ray diffraction (XRD) analysis

XRD (Malvern Panalytical X'Pert^3 Powder X-ray Diffractometer, Netherland) was applied to analyze biotin, POP, and Bio-POP conjugates dried powders. The XRD pattern of samples were measured with X-ray diffractometer which set between 5° to 80° with a scanning range of 2θ.[35]

Thermo-gravimetric (TGA) analysis

The thermal analysis technique (TGA) was applied to investigate the thermal stability of material. Under the stable and controllable conditions, the weight of the material was measured by device in terms of temperature and time. The TGA experiment was performed on a thermal gravimetric instrument (STA 449 F5 Jupiter, Germany) at 25–850 °C under dynamic argon with a heating rate of 10 °C min^{-1}.

Surface morphology analysis

The surface morphology of POP, Bio-POP conjugates was observed by a SEM (Nova Nano SEM 450). Sample of dried powder was adhered to double-sided adhesive carbon tape, metalized with a thin layer of gold and further tested in the microscope operating at 5 kV with a magnification of 10 000×.[36]

In vitro cytotoxicity assay

Cytotoxicity of POP, biotin, and Bio-POP conjugates were evaluated by MTT assay, and the cytotoxicity was replaced by the inhibition concentration IC_{50}. Briefly, HeLa, MCF-7, LO-2, and A549 cells as common and easy-to-cultivable in the assay were applied to research the therapeutic effect on tumour cells of Bio-POP conjugates as one kind of tumour chemotherapy agent *in vitro*. The cytotoxicity of POP, biotin, and Bio-POP conjugates was studied by MTT assay.[37] HeLa, MCF-7, and LO-2 cells were incubated in 96-well plates with 100 μL DMEM medium in a humidified incubator containing 5% CO_2 at 37 °C for 24 h. A549 cells were seeded in 96-well plates in 100 μL of RPMI-1640 medium in a humidified incubator containing 5% CO_2 at 37 °C for 24 h.[38]

Then the cells were cultured in 200 μL medium containing different concentrations of POP, biotin, and Bio-POP conjugates for 48 h. Next, 20 μL of MTT solution (5 mg mL^{-1} in PBS) was added to each well and subsequently incubated for 4 h in a humidified incubator. To terminate the culture at the end of incubation, the culture solution needed to be carefully sucked out of the hole. The collected formazan in 96-well plates was dissolved in dimethyl sulfoxide (200 μL), and then was measured the OD at 490 nm.[39] The samples of 96-well plates were measured three times, and the data were expressed with mean.

$$\text{Viable cells (\%)} = [(\mathrm{OD_{sample}} - \mathrm{OD_{blank}})/(\mathrm{OD_{control}} - \mathrm{OD_{blank}})] \times 100\% \quad (2)$$

where the sample was the presence of the drug, and the blank was the absence of the drug.

Nuclear staining assay

A549 cells were added into 2.00 mL RPMI-1640 medium in a 6-well cell culture plate (Thermo Fisher Scientific), which was incubated in a humidified incubator containing 5% CO_2 at 37 °C for 24 h. Then, A549 cells was dealt with the POP (0 and 480 mg mL^{-1}), biotin (400 and 800 μg mL^{-1}) and Bio-POP conjugates (22 and 44 μg mL^{-1}) solution for 24 h. At the end of the treatment, discarded the supernatant in the 6-well plate, A549 cells were washed with cold PBS and harvested after trypsin treatment. Cells were treated with 4% paraformaldehyde and stained with Hoechst 33342 for 15 min. Ultimately, A549

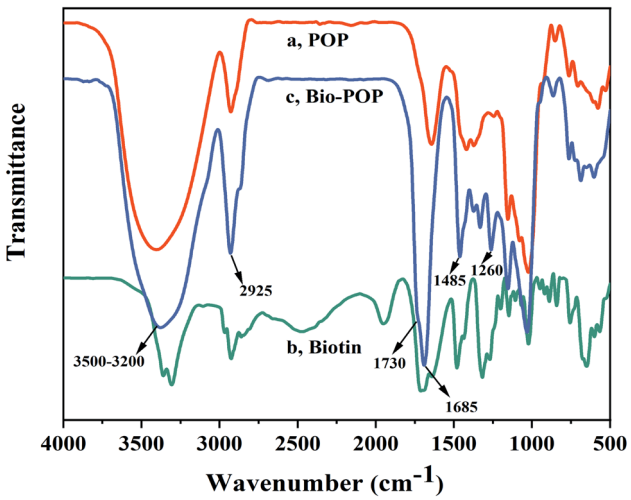

Fig. 2 FT-IR spectra of POP (a), biotin (b), and Bio-POP conjugates (c).

cells were washed twice with cold PBS buffer to remove the probe residue and immediately observed and photographed under an inverted fluorescent microscopy (LEICA M165 FC, Germany).

Cellular immunofluorescence experiment

The immunofluorescence method of the anti-calreticulin antibody was employed in this assay.[40] A549 cells were cultured in RPMI-1640 medium containing 10% fetal bovine serum in a wet air incubator containing 5% CO_2 at 37 °C. When the cells were in the logarithmic growth phase, they were digested with 0.25% trypsin, 80% of the prostheses were digested with RPMI-1640 medium after contraction, and the supernatant was discarded by centrifuged. The precipitate was transferred into cell suspension with the medium, evenly distributed in a 20 mm laser scanning confocal culture dish. When the cell density was

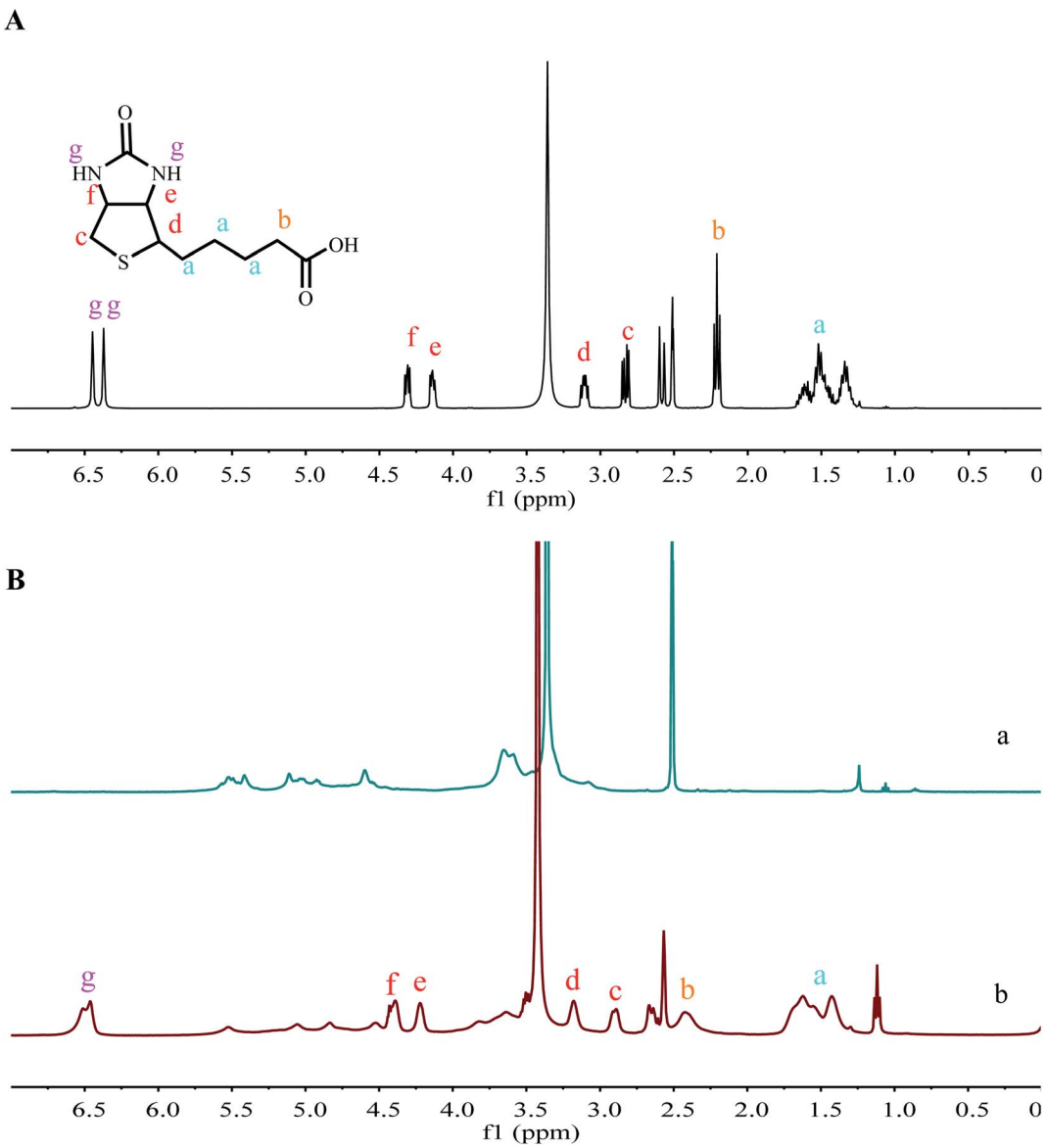

Fig. 3 (A) ^{1}H NMR spectra of biotin in DMSO-d_6; (B) ^{1}H NMR spectra of POP (a) and Bio-POP conjugates (b) in DMSO-d_6.

about 50–60%, the drug was added and the mixture was cultured for 24 h. According to the MTT experiment, the IC_{50} value of each sample was taken as the final concentration.

Then the cells were removed the culture solution, washed with PBS, covered the bottom of the Petri dish with 4% polyformaldehyde and fixed for 20 minutes at room temperature. The cells were permeabilized with 0.1% Triton X-100 for 5 min, washed three times with cold PBS, blocked with 5% BSA for 1 h, and then incubated with the anti-Calreticulin antibody at 1/500. After the first anti incubation, the cells were washed three times/5 min with PBS. Subsequently, the cells were further cultured with a secondary goat antibody to Rabbit IgG (Alexa Fluor® 488) carrying a fluorescent label for 1 h at room temperature, and the nuclei were labeled with DAPI. The whole process needed to be completely dark.[41] Fluorescence images were obtained immediately by ZEISS Laser Scanning Microscope (LMS710, Germany).

3. Results and discussion

FT-IR analysis

The FT-IR spectra of POP, biotin, and Bio-POP conjugates were schematized in Fig. 2. Compared with POP spectra pattern, the peaks of Bio-POP conjugates appeared the stretching vibration of the C=O at about 1730 cm^{-1} which belonged to the stretching vibration absorption peak of the carboxyl of biotin. When biotin reacted with POP, this peak appeared in the infrared spectra, which meant that biotin was grafted onto the POP and successfully bonded to the hydroxyl groups. Meanwhile, the vibration peak of Bio-POP conjugates, such as N–H telescopic vibration overlapped with O–H stretch at 3500–3200 cm^{-1}, stretching vibration band of $-CH_3$ and $-CH_2$ groups around 2925 cm^{-1}, have significantly enhanced. Furthermore, the infrared characteristic peaks at 1685, 1485, and 1260 cm^{-1} were the stretching vibration of the carbonyl group (amide I peak), N–H bending and tensile vibration (amide II peak), and C–N bending vibration (amide III peak),[42,43] which verified biotin successfully grafted with POP through esterification reaction.

^{1}H NMR analysis

The ^{1}H NMR spectra of biotin, POP, and Bio-POP conjugates were exhibited in Fig. 3. In the ^{1}H NMR spectra of POP, the signal peaks at 4.0–5.0 ppm and 5.0–5.6 ppm respectively belonged to beta configuration and alpha configuration. Besides, the ^{1}H NMR peaks of biotin did not appear in the range of 4.5–5.3 ppm. If a ^{1}H NMR signal appears in this area, it belongs to *Portulaca oleracea* polysaccharides. Compared with the ^{1}H NMR spectrum of *Portulaca oleracea* polysaccharides, the hydroxyl peak of Bio-POP conjugates at 4.60–5.40 ppm decreased significantly, and the inherent peak of POP was retained. A new nuclear magnetic resonance peak appeared in the ^{1}H NMR spectrum of Bio-POP conjugates: 1.29–1.66 ppm ($-CH_2CH_2CH_2-$), 2.33 ppm ($-OOCCH_2-$), 2.57–2.89 ppm ($-S-CH_2-$), 4.17 ppm (S–CH–),[44] 4.32 ppm ($-S-CH_2-CH$), and 6.46 ppm (–NH–CO), 6.51 ppm (–NH–CO).[45,46] Therefore, both ^{1}H NMR and FT-IR spectra confirmed that biotin was successfully grafted onto *Portulaca oleracea* polysaccharides by CDI activation.

Degree of substitution analysis

An inductively coupled plasma spectrometer is an analytical method for the simultaneous determination of multiple elements, which analysis features are high sensitivity and high analysis speed. It is widely used in the qualitative and quantitative analysis of inorganic elements such as biological medicine, food, soil, rock, *etc.* In this experiment, the degree of substitution of biotin was further derived according to the formula eqn (1) by measuring the sulfur content in two sets of parallel purified products. The product was an off-white powder with an average degree of substitution of 42.5.

XRD analysis

XRD analysis was performed on all samples to prove that biotinylated *Portulaca oleracea* polysaccharides were synthesized by covalent bonding. Fig. 4 displayed the X-ray diffraction (XRD) pattern of the POP, biotin, and Bio-POP conjugates, and the

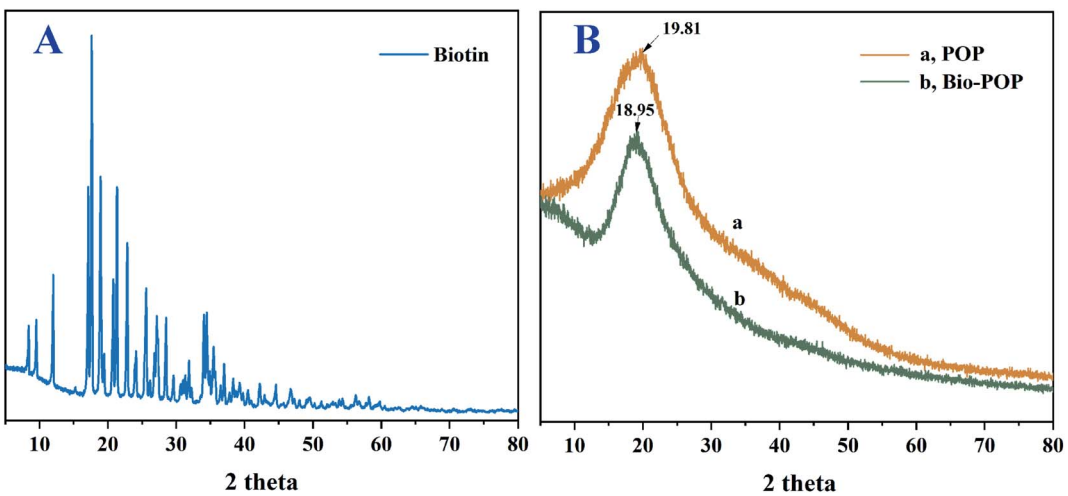

Fig. 4 (A) XRD spectra of biotin; (B) XRD spectra of POP (a) and Bio-POP conjugates (b).

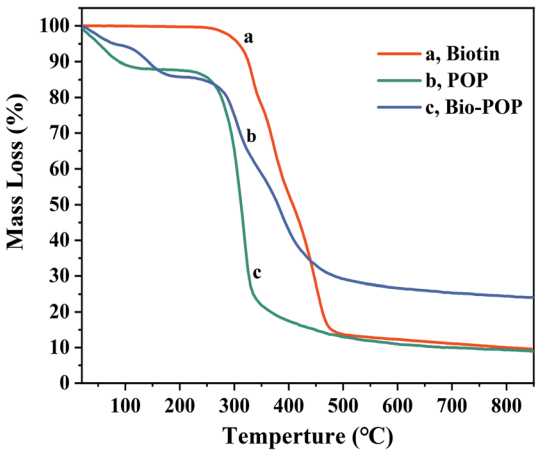

Fig. 5 TGA thermograms of biotin (a), POP (b) and Bio-POP conjugates (c) measured at 25 °C.

XRD result illustrated biotin had nine typical crystal peaks at 2θ of 8.3°, 9.4°, 11.9°, 17.6°, 18.9°, 21.3°, 22.7°, 28.4°, 34.3° and many small mountains between 30° and 60°. Therefore, the degree of crystallinity of biotin was high.[47,48] There were many crystal diffraction peaks in the biotin spectrum, then POP had only one diffraction peak, which was a broad and diffuse diffraction peak at 2θ of 19.81°. Relative to POP, the spectrum diffraction peak of Bio-POP conjugates was slightly shifted at 2θ of 18.95°. The above confirmed that the crystal structure of biotin was disrupted after the esterification reaction, and verified the Bio-POP conjugates were successfully synthesized.

TGA analysis

The TGA curves of POP, biotin, and Bio-POP conjugates were measured in the temperature range of 20–850 °C, as exhibited in Fig. 5. Firstly, biotin had a significant mass loss at 257–495 °C, which was caused by the decomposition of biotin. POP and Bio-POP conjugates had a small mass loss below 160 °C owing to the loss of bonding water in the sample. Secondly, when the temperature was 250–500 °C, the mass loss rate of POP and Bio-POP conjugates was the highest. Compared with the TGA curves of POP and Bio-POP conjugates in this stage, the thermal decomposition rate of Bio-POP conjugates was significantly slower than that of POP, which was due to the depolymerization and decomposition of polysaccharides and some ester bonds. Finally, when heated to 850 °C, the Bio-POP conjugate had the least heat loss. From the above analysis results, the grafting of *Portulaca oleracea* polysaccharides with biotin greatly improved the thermal stability of the conjugates.

SEM analysis

The effect of biotin modification on the physical morphology of polysaccharides was determined by scanning electron microscopy (SEM). The SEM image of *Portulaca oleracea* polysaccharides had a smooth and dense layered structure on the surface morphology as shown in Fig. 6(A), which was related to the freeze-drying method of purified polysaccharides. The structure of agglomerated particles of Bio-POP conjugates was significantly different from that of POP, and the morphology of Bio-POP conjugates was a loose and porous cross-linked structure, as revealed in Fig. 6(B). The carboxyl group reacted with the hydroxyl group to form the ester group, which enhanced hydrophobicity, while the hydrophobic biotin and the hydrophilic *Portulaca oleracea* polysaccharides formed pores through the ester bond, which was conducive to grafting more biotin.

Cytotoxicity and anti-cancer activity

The cytotoxicity of biotin, POP, and Bio-POP conjugates, replacing by half maximal inhibitory concentration (IC_{50}), was measured by MTT assay as shown in Fig. 7. The potential value of medicine of Bio-POP conjugates as anti-cancer drug was evaluated using HeLa, MCF-7, LO-2, and A549 cell lines *in vitro*. The results were shown in Fig. 7, which illustrated that Bio-POP conjugates restricted the cell activity of HeLa, MCF-7, LO-2, and A549 cell lines. IC_{50} values of Bio-POP conjugates were 64.3, 60.2, 61.9, and 43.6 μg mL^{-1} respectively for HeLa, MCF-7, LO-2 and A549 cell lines. Thus, the effect of Bio-POP conjugates on A549 cells was more obvious.

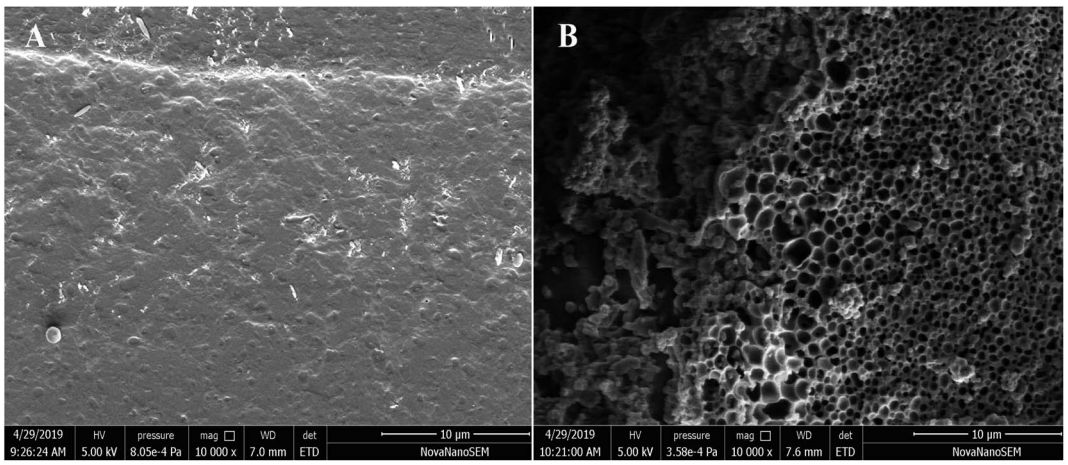

Fig. 6 SEM images of POP (A) and Bio-POP conjugates (B): (A) 10 000×; (B) 10 000×.

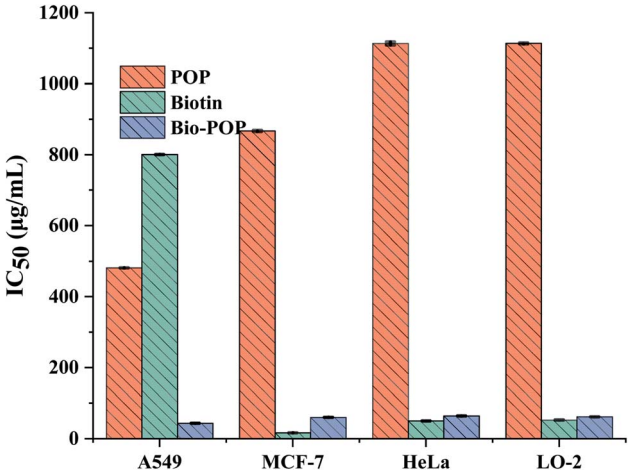

Fig. 7 IC_{50} value of A549, MCF-7, HeLa and LO-2 cells treated with biotin, POP and Bio-POP conjugates for 48 h.

On the other hand, it was reported that *Portulaca oleracea* polysaccharides had antitumor activity, which was consistent with our test results. POP had little effect on the four cell lines, which IC_{50} values was 1113.3, 867.1, 1113.4, and 481.4 μg mL^{-1} respectively for HeLa, MCF-7, LO-2 and A549 cell lines, but POP inhibited the growth of A549 cell line than other cell lines. The IC_{50} values of biotin were 50.1, 16.57, 52.7, and 800.4 μg mL^{-1} respectively for HeLa, MCF-7, LO-2 and A549 cell lines, which confirmed that biotin had little effect on the growth of A549 cells. Comparing the IC_{50} values of the four cell lines, it was found that POP had more toxicity to A549 cells, while biotin had less toxicity to A549 cells. Therefore, the selection of A549 cells as the research cell lines of subsequent biological experiments can better reflect the synergistic anti-cancer effect of polysaccharides. In general, Bio-POP conjugates can be used as drug carriers.

Fluorescent microscopic analysis for the detection of apoptosis

Fig. 8 exhibited the cellular nuclear morphology of A549 cells stained by Hoechst 33342 and observed under a fluorescence microscope. The nuclear fluorescent staining Hoechst 33342 was applied to specifically staining the nuclear of living cells which could penetrate cell membranes and embed it into double-stranded DNA to release blue fluorescence. It can enter the normal cell membrane a little and make it stained with low blue. However, owing to the enhanced cell membrane permeability of apoptotic cells, the number of Hoechst 33342 entering apoptotic cells was significantly higher than that of healthy cells, and the fluorescence intensity was also higher than that of healthy cells. Therefore, the effect of biotin, POP, and Bio-POP conjugates on apoptosis was studied.[49]

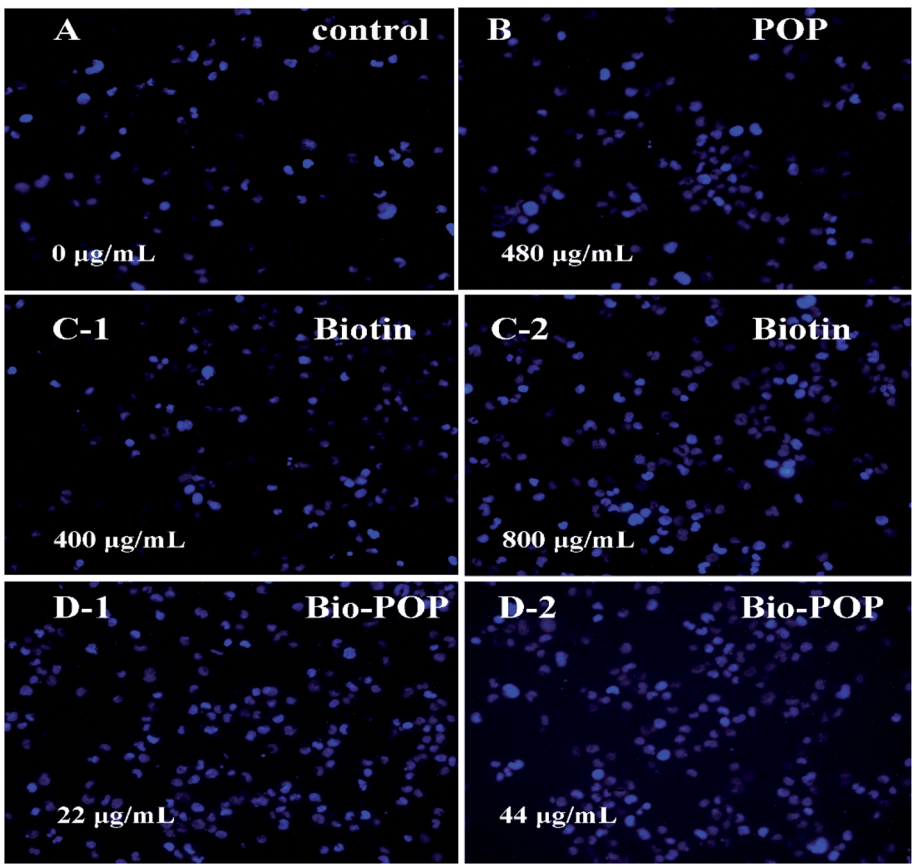

Fig. 8 Fluorescence microscopic images showing morphological changes in the nuclei of A549 cells treated with (A) control 0 μg mL^{-1}, (B) POP 480 μg mL^{-1}, (C) biotin 400 and 800 μg mL^{-1}, and (D) Bio-POP conjugates 22 and 44 μg mL^{-1}.

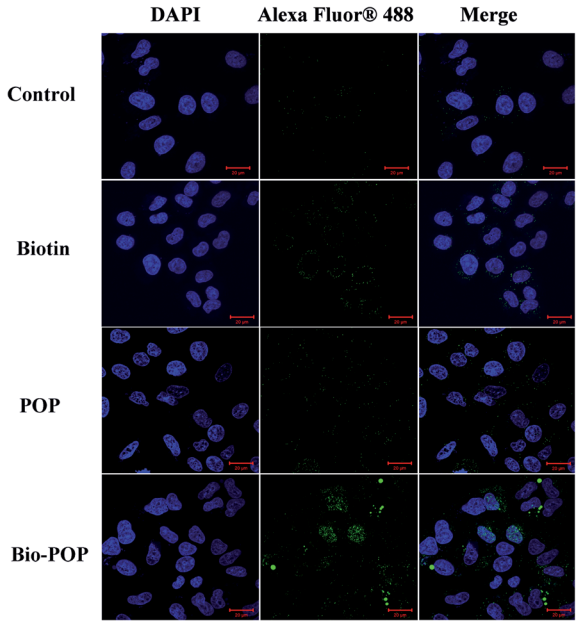

Fig. 9 Images of A549 cells after incubation with POP, biotin, and Bio-POP conjugates for 24 h. Scale bar represents 20 μm.

In the control group, the cells showed blue fluorescence and a regular round shape. The nucleus morphology after treatment with different concentrations of biotin and POP was similar to that of the control group, indicating that the effect of biotin and POP on cell apoptosis was weak. Nevertheless, A549 cells were treated with Bio-POP conjugates at different dilution concentration ratio for 24 h. The number of condensed nuclei increased significantly and the nuclei were fragmented,[50] which illustrated the apoptosis of A549 cells was induced by Bio-POP conjugates.

The distribution of CRT in A549 cells

The results of the cellular immunofluorescence experiment were exhibited in Fig. 9. Calreticulin (CRT) is a highly conserved multifunctional protein, which is widely distributed in the nucleus, cell membrane, endoplasmic reticulum and extracellular matrix.[51] The clinical and laboratory data indicated that CRT was closely related to the occurrence and development of tumors. Membrane CRT mediated the immunogenic death of tumour cells. CRT on the surface of apoptotic cells could assist the body to clear apoptotic cells and participate in the immunogenic death.[52] When the cells occurred apoptosis, CRT transferred to cell membrane. Some chemotherapeutics (anthracycline, oxaliplatin, *etc.*) can promote the apoptosis of tumour cells and enhance its immunogenicity. CRT could express in normal cells, tumour cells, apoptotic cells, and some drug-treated cells.

A549 cells were treated with drugs, and the expression of calreticulin in A549 cells was detected by immunofluorescence assay. CRT was expressed in A549 cells of the control group as shown in Fig. 9, which was mainly located in the intracellular. When A549 cells were stimulated by immune drugs, CRT was transferred from intracellular to the outermost layer of the cell membrane and even to the extracellular matrix. POP had regulatory immune activity, and the normal operation of many immune cells also needed biotin. Therefore, the expression of calreticulin (green fluorescence) in the control group, biotin, and Bio-POP conjugates increased in turn. In conclusion, the extracellular release of calreticulin was observed in Fig. 9, indicating that the Bio-POP conjugates had immunoregulatory properties.

4. Conclusion

In conclusion, the composition of Bio-POP conjugates was the biotin anchored POP by covalent bonds. Infrared and magnetic resonance spectrometry indicated that biotin successfully grafted onto POP. The crystal structure of biotin was destroyed by esterification, and Bio-POP conjugates were also amorphous by the profiles of XRD. The polymeric carrier containing biotin was expected to recognize tumor surface receptors and transfect cells through receptor-mediated endocytosis. In MTT assay, biotin had relatively little effect on the proliferation of A549 cells, while Bio-POP conjugates had an obvious effect on the proliferation of A549 cells. The results of the MTT experiment illustrated that the Bio-POP conjugates could inhibit cell proliferation more than POP.

Combined with cellular nuclear staining experiment, Bio-POP conjugates could significantly damage the cellular nuclear of A549 cells. The increase of expression quantity of calreticulin in A549 cells treated with Bio-POP conjugates was detected by immunofluorescence comparing with POP. The synergistic effect of immune means and chemotherapy drugs inhibited tumor cell proliferation. Polysaccharide drug system based on *Portulaca oleracea* polysaccharides were modified by biotin and applied to drug coupling materials. The purpose of this study was to provide a simple idea for the functional modification of *Portulaca oleracea* polysaccharides so that it was applied in clinical production of more polysaccharides drug conjugates.

Conflicts of interest

The authors declare no competing financial interest.

Acknowledgements

This work was supported by the National Natural Science Foundation of China (Project no. 21571154), the “Six Talent Peaks Project” in Jiangsu Province, the Jiangsu Fundament of “Qinglan Project” and “333 Project”.

References

1 X. F. Liu, X. Q. Wang, X. F. Xu and X. W. Zhang, *Int. J. Biol. Macromol.*, 2019, **127**, 39–47.
2 H. Ranji-Burachaloo, P. A. Gurr, D. E. Dunstan and G. G. Qiao, *ACS Nano*, 2018, **12**, 11819–11837.
3 Z. Y. Yang, J. Xu, Q. Fu, X. L. Fu, T. Shu, Y. P. Bi and B. Song, *Carbohydr. Polym.*, 2013, **95**, 615–620.
4 A. S. Kritchenkov, A. R. Egorov, N. V. Dubashynskaya, O. V. Volkova, L. A. Zabodalova, E. P. Suchkova,

A. V. Kurliuk, T. V. Shakola and A. P. Dysin, *Int. J. Biol. Macromol.*, 2019, **134**, 480–486.
5 Z. Y. Zhu, X. C. Liu, X. N. Fang, H. Q. Sun, X. Y. Yang and Y. M. Zhang, *Int. J. Biol. Macromol.*, 2016, **82**, 959–966.
6 Y. G. Chen, Z. J. Shen and X. P. Chen, *Int. J. Biol. Macromol.*, 2009, **45**, 448–452.
7 S. R. Fan, J. F. Zhang, W. J. Nie, W. Y. Zhou, L. Q. Jin, X. M. Chen and J. X. Lu, *Food Chem. Toxicol.*, 2017, **102**, 53–62.
8 S. Nisar, A. H. Pandit, L. Wang and S. Rattan, *RSC Adv.*, 2020, **10**, 14694–14704.
9 M. Kong, X. Peng, H. Cui, P. Liu, B. Pang and K. Zhang, *RSC Adv.*, 2020, **10**, 4860–4868.
10 M. Rahbar, A. Morsali, M. R. Bozorgmehr and S. A. Beyramabadi, *J. Mol. Liq.*, 2020, **302**, 112495.
11 I. Brigger, C. Dubernet and P. Couvreur, *Adv. Drug Delivery Rev.*, 2012, **64**, 24–36.
12 H. Wang, H. Hu, H. Yang and Z. Li, *RSC Adv.*, 2021, **11**, 3226–3240.
13 F. Bai, Y. Wang, Q. Q. Han, M. L. Wu, Q. Luo, H. M. Zhang and Y. Q. Wang, *J. Mol. Liq.*, 2019, **288**, 111079.
14 M. A. Wsoo, S. Shahir, S. P. Mohd Bohari, N. H. M. Nayan and S. I. A. Razak, *Carbohydr. Res.*, 2020, **491**, 107978.
15 Y. Y. Zheng, J. Monty and R. J. Linhardt, *Carbohydr. Res.*, 2015, **405**, 23–32.
16 M. H. Lee, Z. G. Yang, C. W. Lim, Y. H. Lee, S. Dongbang, C. Kang and J. S. Kim, *Chem. Rev.*, 2013, **113**, 5071–5109.
17 M. Gangopadhyay, R. Mengji, A. Paul, Y. Venkatesh, V. Vangala, A. Jana and N. D. P. Singh, *Chem. Commun.*, 2017, **53**, 9109–9112.
18 J. S. Butler and P. J. Sadler, *Curr. Opin. Chem. Biol.*, 2013, **17**, 175–188.
19 G. H. Hou, J. M. Qian, W. J. Xu, T. T. Sun, Y. P. Wang, J. L. Wang, J. L. Ji and A. L. Suo, *Carbohydr. Polym.*, 2019, **212**, 334–344.
20 Y. Q. Li, Y. K. Hu, S. J. Shi and L. Jiang, *Int. J. Biol. Macromol.*, 2014, **68**, 113–116.
21 A. Sharma, G. Kaithwas, M. Vijayakumar, M. K. Unnikrishnan and C. V. Rao, *J. Food Biochem.*, 2012, **36**, 378–382.
22 Y. P. Li, L. H. Yao, G. J. Wu, X. F. Pi, Y. C. Gong, R. S. Ye and C. X. Wang, *Food Sci. Biotechnol.*, 2014, **23**, 2045–2052.
23 C. X. Dong, K. Hayashi, J. B. Lee and T. Hayashi, *Chem. Pharm. Bull.*, 2010, **58**, 507–510.
24 F. Y. Gong, F. L. Li, L. L. Zhang, J. Li, Z. Zhang and G. Y. Wang, *Int. J. Mol. Sci.*, 2009, **10**, 880–888.
25 Y. Q. Li, Y. K. Hu, S. J. Shi and L. Jiang, *Int. J. Biol. Macromol.*, 2014, **68**, 113–116.
26 Y. N. Georgiev, M. H. Ognyanov, H. Kiyohara, T. G. Batsalova, B. M. Dzhambazov, M. Ciz, P. N. Denev, H. Yamada, B. S. Paulsen, O. Vasicek, A. Lojek, H. Barsett, D. Antonova and M. G. Kratchanova, *Int. J. Biol. Macromol.*, 2017, **105**, 730–740.
27 K. B. Oh, I. M. Chang, K. J. Hwang and W. Mar, *Phytother. Res.*, 2000, **14**, 329–332.
28 H. Shen, G. Tang, G. Zeng, Y. J. Yang, X. W. Cai, D. L. Li, H. C. Liu and N. X. Zhou, *Carbohydr. Polym.*, 2013, **93**, 395–400.
29 S. Maiti and P. Paira, *Eur. J. Med. Chem.*, 2018, **145**, 206–223.
30 E. Esposito, I. Vlodavsky, U. Barash, G. Roscilli, F. M. Milazzo, G. Giannini and A. Naggi, *Eur. J. Med. Chem.*, 2020, **186**, 111831.
31 B. Q. Xiong, C. H. Hu, H. T. Li, C. S. Zhou, P. L. Zhang, Y. Liu and K. W. Tang, *Tetrahedron Lett.*, 2017, **58**, 2482–2486.
32 J. Liu, X. C. Wang, H. M. Yong, J. Kan, N. F. Zhang and C. H. Jin, *Int. J. Biol. Macromol.*, 2018, **114**, 130–136.
33 Y. Y. Yu, Y. J. Zhang, C. B. Hu, X. Y. Zou, Y. Lin, Y. Y. Xia and L. J. You, *Food Chem. Toxical.*, 2019, **128**, 119–128.
34 Y. Q. Wang, Q. Q. Han, Y. Wang, D. Qin, Q. Luo and H. M. Zhang, *Colloids Surf., A*, 2020, **597**, 124763.
35 J. N. Putro, S. Ismadji, C. Gunarto, F. E. Soetaredjo and Y. H. Ju, *Colloids Surf., A*, 2019, **578**, 123618.
36 L. S. Lai and D. H. Yang, *Food Hydrocolloids*, 2007, **21**, 739–746.
37 Q. Q. Qian, S. W. Niu, G. R. Williams, J. R. Wu, X. Y. Zhang and L. M. Zhu, *Colloids Surf., A*, 2019, **564**, 122–130.
38 S. Buwalda, B. Nottelet, A. Bethry, R. J. Kok, N. Sijbrandi and J. Coudane, *J. Colloid Interface Sci.*, 2019, **535**, 505–515.
39 Y. Wang, Q. Q. Han, F. Bai, Q. Luo, M. L. Wu, G. Song, H. M. Zhang and Y. Q. Wang, *J. Inorg. Biochem.*, 2020, **205**, 111001.
40 J. Tsalikis, M. Abdel-Nour, A. Farahvash, M. T. Sorbara, S. Poon, D. J. Philpott and S. E. Girardin, *Mol. Cell. Biol.*, 2019, **39**, 1–41.
41 J. J. Ou, Y. Peng, W. W. Yang, Y. Zhang, J. Hao, F. Li, Y. R. Chen, Y. Zhao, X. Xie, S. Wu, L. Zha, X. Luo, G. F. Xie, L. T. Wang, W. Sun, Q. Zhou, J. J. Li and H. J. Liang, *Nat. Commun.*, 2019, **10**, 1–14.
42 Q. Luo, Y. Wang, Q. Q. Han, L. S. Ji, H. M. Zhang, Z. H. Fei and Y. Q. Wang, *Carbohydr. Polym.*, 2019, **209**, 266–275.
43 Y. Q. Wang, A. Pitto-Barry, A. Habtemariam, I. Romero-Canelon, P. J. Sadler and N. P. Barry, *Inorg. Chem. Front.*, 2016, **3**, 1058–1064.
44 D. J. Tong, J. Yao, H. R. Li and S. J. Han, *J. Appl. Polym. Sci.*, 2006, **102**, 3552–3558.
45 S. Y. Kim, S. H. Cho, Y. M. Lee and L. Y. Chu, *Macromol. Res.*, 2007, **15**, 646–655.
46 F. E. Chen, H. Q. Jia, X. X. Chen, H. F. Da, B. Xie, Y. Y. Kuang and J. F. Zhao, *Chem. Pharm. Bull.*, 2005, **53**, 743–746.
47 W. Z. Yang, M. M. Wang, L. L. Ma, H. Y. Li and L. Huang, *Carbohydr. Polym.*, 2014, **99**, 720–727.
48 I. S. Kim and I. J. Oh, *Arch. Pharmacal Res.*, 2010, **33**, 761–767.
49 X. B. Zhao, L. Liu, X. R. Li, J. Zeng, X. Jia and P. Liu, *Langmuir*, 2014, **30**, 10419–10429.
50 S. U. Parsekar, J. Fernandes, A. Banerjee, O. P. Chouhan, S. Biswas, M. Singh, D. P. Mishra and M. Kumar, *J. Biol. Inorg Chem.*, 2018, **23**, 1331–1349.
51 S. Johnson, M. Michalak, M. Opas and P. Eggleton, *Trends Cell Biol.*, 2001, **11**, 122–129.
52 A. Tesniere, L. Apetoh, F. Ghiringhelli, N. Joza, T. Panaretakis, O. Kepp, F. Schlemmer, L. Zitvogel and G. Kroemer, *Curr. Opin. Immunol.*, 2008, **20**, 504–511.